JACS
JOURNAL OF THE AMERICAN CHEMICAL SOCIETY
Article
pubs.acs.org/JACS

Real-Time Measurement of the Vertical Binding Energy during the Birth of a Solvated Electron

Julia Stähler,* Jan-Christoph Deinert, Daniel Wegkamp, Sebastian Hagen, and Martin Wolf

Abteilung Physikalische Chemie, Fritz-Haber-Institut der Max-Planck-Gesellschaft, Faradayweg 4-6, 14195 Berlin, Germany

ABSTRACT: Using femtosecond time-resolved two-photon photoelectron spectroscopy, we determine (i) the vertical binding energy (VBE = 0.8 eV) of electrons in the conduction band in supported amorphous solid water (ASW) layers, (ii) the time scale of ultrafast trapping at pre-existing sites (22 fs), and (iii) the initial VBE (1.4 eV) of solvated electrons *before* significant molecular reorganization sets in. Our results suggest that the excess electron dynamics prior to solvation are representative for bulk ASW.

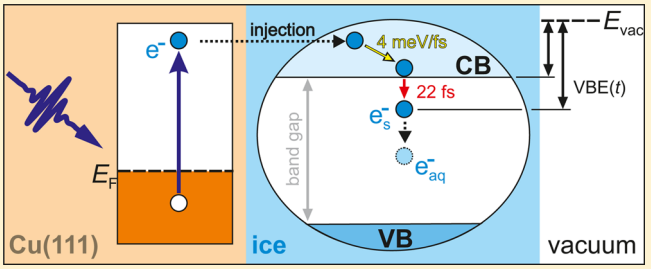

INTRODUCTION

Excess electrons in aqueous environments play a crucial role in physics, chemistry, and biology, not least due to the importance of water as the paramount solvent in nature.[1,2] The alignment of energy levels of solute molecules with respect to the affinity level of water plays a crucial role in charge-transfer reactions, as it determines the probability of solvated electron (SE) formation. Thereby, an excess electron is stabilized by the polar, aqueous surroundings. SEs are known to be highly reactive species, for example, in dissociative electron attachment,[3] ammonia synthesis,[4] and CO_2 reduction in water[5] or ice[6] solutions.

One way of looking at the energy levels of water is by interpreting it as an amorphous large-band-gap semiconductor with an occupied valence band (VB) and unoccupied conduction band (CB). The transport of electrons is then determined by the band dispersion and competing decay channels, like localization and trapping of the charge carriers. A negatively charged electron−water complex can then be considered to be an anionic defect of pure water.[7] The injection of electrons requires energetic resonance of the donor level with the water CB; for electron-induced chemical reactions, the relaxed water−electron complex $(H_2O)^-$ must be in resonance with accepting states of the reactant. The vertical binding energies (VBEs) of these energy levels are difficult to determine directly for liquid water. This led to numerous experimental and theoretical studies on water anion clusters in the gas phase,[8−12] aiming at the extrapolation of VBEs to the bulk value.

When discussing the solvation dynamics of excess electrons in an aqueous environment, it is helpful to consider the energy levels in a Marcus type of picture (cf. Figure 1a), where the total energy consists of the binding energy of the electron and the reorganization energy stored in the distorted solvent. In the case of neutral water (H_2O, orange curve), the electron is still in the VB, and formation of the (empty) solvation shell requires the reorganization energy λ_{aq}. As shown by scavenger experiments[13] and, very recently, by time-resolved (TR) terahertz (THz) spectroscopy,[14] photoexcitation to the CB first creates a delocalized excess electron, $(H_2O)^-_{deloc}$ (dark blue curve). This excess electron[15] gains considerable binding energy by localization in the solvation shell, $(H_2O)_{loc}$, and thereby compensates λ_{aq}; the total energy is minimized at q_0. The vertical binding energy of such *relaxed* SEs, VBE_{aq}, was determined by TR photoelectron (PE) spectroscopy for both liquid water (bulk, 3.3 eV; surface, 1.6 eV)[16,17] and ice crystallites (surface, 3.8 eV).[18,19] Despite numerous studies, however, the VBE of the water CB remains unknown. The reason for this is the ultrashort lifetime of electrons in this delocalized state, as localization through electron solvation is energetically much more favorable. Due to the rapidness of this process, neither the localization dynamics nor the mechanism (small polaron formation by self-trapping versus localization at pre-existing potential minima) could be resolved until now.

Besides time resolution, one main experimental challenge for this particular question is the controlled injection of electrons into the water CB and their subsequent probing by TR spectroscopy, which can be solved by photoexcitation of, e.g., H_2O itself or ions in solution.[13,17] However, the formation dynamics of SEs are influenced by the presence of the positively charged donor. A complementary approach that does not involve positively charged ions in the vicinity of the SE involves the injection of electrons from a metallic or semiconducting substrate. This can be performed at solid−liquid interfaces[4,5] and also in adsorbed amorphous solid water (ASW) layers.[20−23] It was shown that the excess electrons are transferred to a localized SE state, e_S. Rearrangement of the water molecules leads to a continuous binding energy increase, while the electron−ice complex moves toward its new equilibrium position and its population reduces due to competing decay to the metal substrate.[21,23] These SEs are localized in the second−third ice bilayer (BL) in front of the metal template.[22] Despite these previous studies, (i) the VBE of the ice CB, (ii)

Received: November 17, 2014
Published: January 22, 2015

DOI: 10.1021/ja511571y
J. Am. Chem. Soc. 2015, 137, 3520−3524

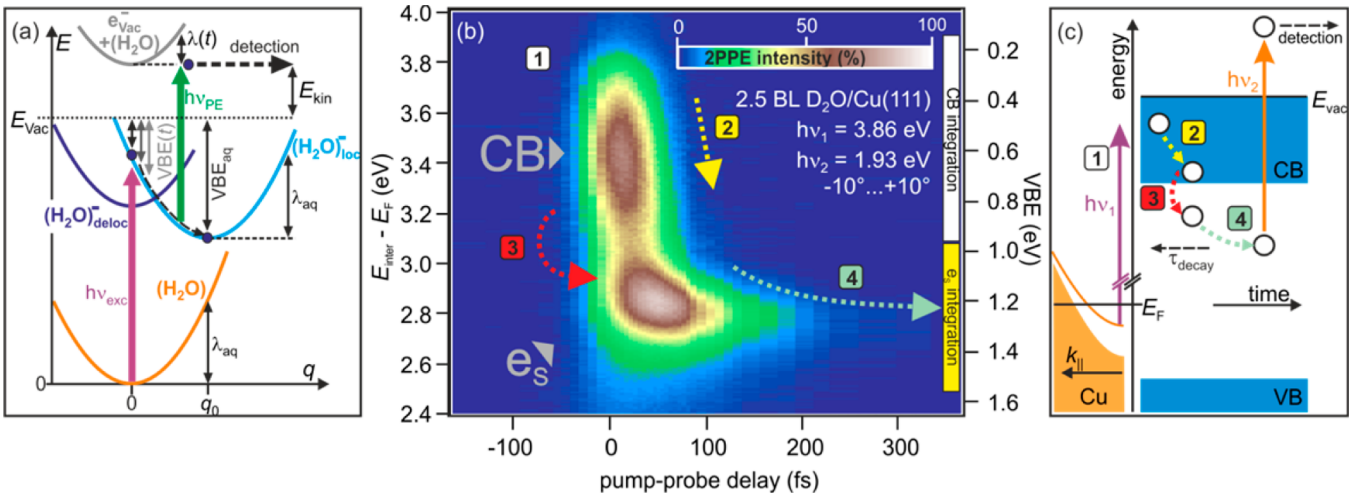

Figure 1. (a) Marcus parabolas for solvated electrons in water/ice and time-resolved photoelectron spectroscopy scheme. (b) Angle-integrated two-photon photoelectron intensity of amorphous solid water on Cu(111) as a function of energy and pump−probe time delay. (c) Indicated elementary processes: (1) metal electron injection into the ice conduction band, (2) relaxation to the band minimum on fs time scales, (3) e_S population, and (4) energetic stabilization and population decay to the metal substrate.

the time scale of electron localization, and (iii) the fundamental question of whether the excess electrons get trapped by small polaron formation or if they localize at pre-existing trapping sites remain unanswered.

In this Article, we present femtosecond TR two-photon photoelectron (2PPE) experiments with significantly improved time resolution compared to previous work that allows for a clear assignment of all involved processes on the electron's passage through the ice CB of ASW grown on a Cu(111) template. Figure 1c illustrates all the elementary processes: The electrons are photoexcited from a (through D_2O adsorption) strongly broadened Cu(111) surface state (SS) into the continuum of ice CB states (1), before they rapidly relax with a remarkably high rate of 4 meV/fs toward the bottom of the CB (2), which lies at a VBE of 0.8 eV. The carriers are then trapped in pre-existing, localized traps with a characteristic time constant of 22 fs (3) and are subsequently stabilized energetically by rearrangement of the ice network (4). This first real-time measurement of excess electron dynamics in and out of the CB of an aqueous solvent provides unprecedented knowledge of the initial steps of SE formation.

EXPERIMENTAL SECTION

The ASW formed by D_2O[24] is *in situ* grown onto a Cu(111) single-crystal surface at 90 K, prepared under ultrahigh-vacuum conditions by Ar^+ sputtering and annealing cycles as described elsewhere in detail.[21] The coverage of 2.5(5) BL is determined by a combination of thermal desorption spectroscopy and the measurement of the sample work function (Φ = 4.05(5) eV) at the low-energy cutoff of the PE spectra (see, e.g., ref 25 for details). For TR 2PPE spectroscopy, the output of a regeneratively amplified laser system (40 fs at 800 nm and a repetition rate of 200 kHz) is used to drive an optical parametric amplifier that provides the pump and probe pulses with $h\nu_1$ = 3.86 eV and $h\nu_2$ = 1.93 eV, respectively. The cross correlation of the two laser pulses is measured independently by TR 2PPE of the occupied Cu(111) SS via virtual intermediate states (see, e.g., ref 26 for details), leading to a mean pulse duration of 35(5) fs. The time resolution is determined by the accuracy of time-zero determination (5 fs).[27]

As sketched in Figure 1c, $h\nu_1$ launches the non-equilibrium dynamics in the sample by populating normally unoccupied states above E_F, while $h\nu_2$ photoemits the excited electron population above E_{vac}. The kinetic energy of these photoelectrons is detected by a hemispherical electron analyzer. As the photon energies and work function of the sample are known, the PE intensity distribution can be plotted as a function of initial state energy below the Fermi energy, $E_{initial} - E_F = E_{kin} + \Phi - (h\nu_1 + h\nu_2)$, intermediate state energy above it, $E_{inter} - E_F = E_{kin} + \Phi - h\nu_2$, or VBE = $h\nu_2 - E_{kin}$. The energy resolution of the experiment is 60 meV.

RESULTS AND DISCUSSION

Figure 1b shows the time-dependent 2PPE intensity of ASW on Cu(111) integrated over ±10° emission angle in a false color representation as a function of intermediate state (left axis) and vertical binding energy (right axis). The spectrum exposes two features: (i) a broad peak at large energies (VBE = 0.4−0.8 eV), quickly shifting toward larger VBE and rapidly losing intensity, and (ii) a sharper maximum (VBE = 1.1−1.3 eV) that exhibits a delayed intensity rise, a longer lifetime, and a comparably slow shift to larger binding energy. In agreement with our previous work,[21−23] we assign the former to the ice CB and the latter to SEs in the ice, which are energetically stabilized by their dipolar environment. However, contrary to the previous studies, the improved time resolution of our experiment now enables the first clear distinction among *all* involved elementary processes: (1) quasi-instantaneous population of the ice CB upon photoexcitation from occupied metal states, (2) electron relaxation in the ice CB, (3) localization and population of e_S, and (4) the previously thoroughly characterized stabilization and decay dynamics of the e_S population. In particular, processes (1)−(3) will be analyzed in detail in the following.

Due to its large band gap, D_2O is transparent to the pump laser light, which is only absorbed in the metal substrate. The well-known projected surface electronic band structure of the Cu(111) surface is sketched in Figure 1c. The free-electron-like Shockley SS of Cu(111) is located in the projected band gap above the projected copper sp band (orange-shaded area). The resulting 2PPE spectrum of the pristine surface is depicted in Figure 2 (orange trace) and plotted as a function of initial state energy. The SS has a binding energy of 400 meV with respect to E_F on pristine Cu(111) (vertical dashed line), which can be subject to modifications when D_2O molecules bind to surface atoms. Comparison of the 2PPE spectrum of the pristine Cu(111) with the one with ASW (blue trace) shows that D_2O adsorption clearly broadens the SS intensity distribution and

DOI: 10.1021/ja511571y
J. Am. Chem. Soc. 2015, 137, 3520−3524

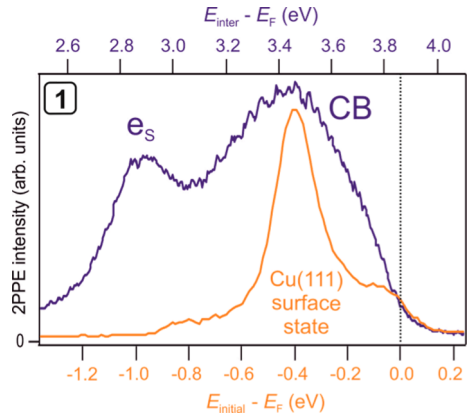

Figure 2. Angle-integrated 2PPE intensity of pristine Cu(111) (orange) and 2.5 BL D_2O/Cu(111) (blue) as a function of initial (bottom axis) and intermediate state energy (top axis). The occupied SS is projected into the CB by $h\nu_1$.

shifts its maximum to slightly lower energies.[28] As the bulk of the copper crystal does not provide any initial states at these energies for the excited electrons in the ice CB, we conclude that excitation must occur directly (resonantly) at the D_2O–Cu interface from a modified Cu(111) SS (elementary step (1) in Figure 1c).

The quasi-instantaneous injection of carriers from the Cu(111) surface into the ASW layer is followed by relaxation of the excess electrons within the ice. Figure 3a depicts 2PPE spectra at different pump–probe time delays. Clearly, the maxima of both spectral signatures, the ice CB and e_S, shift toward larger VBE as time proceeds, as indicated by the arrows. The peak positions are determined by an empirical fit of two Gaussians on top of a linear background (not shown). They are plotted as a function of time delay in Figure 3b and unveil the ultrafast shift of the CB population (blue/yellow) to larger VBE with a rate of 4 meV/fs (process (2) in Figure 1c). We define the VBE(CB) = 0.8(2) eV as the maximum of the photoelectron distribution before its population has decayed.[29] Further, the spectral signature of the SEs, e_S, also shifts to larger binding energies starting at VBE(e_S) = 1.4 eV, but at a significantly lower rate. For comparison, we show the stabilization rate of 0.27 meV/fs observed previously[21] (Figure 3b, green line), which coincides well with the present results. This energetic stabilization results from the dynamic rearrangement of the molecules in the solvation shell and was discussed in detail in our previous work.[21−23,34,35] It should be noted that, for ASW adsorbed on metal surfaces, the competing population transfer to the substrate quenches the population of the e_S state *before* solvation is completed. The final VBE of e_S is significantly larger than the 1.4 eV observed here.

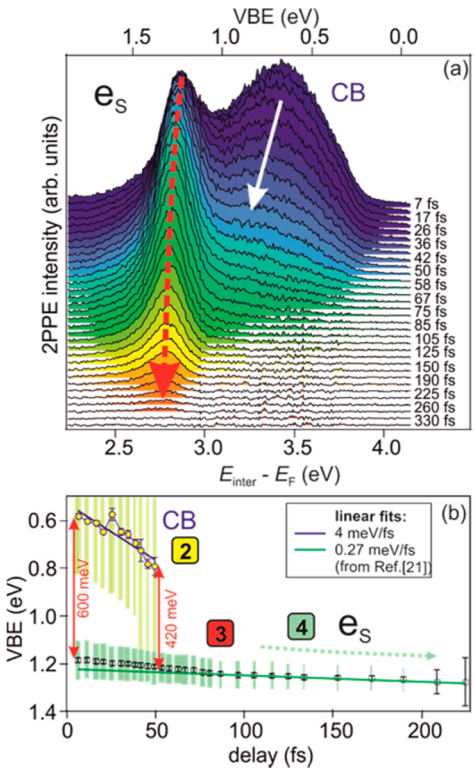

Figure 3. (a) Angle-integrated 2PPE spectra at different pump–probe time delays. The energy shift of CB and e_S is visualized by the arrows. (b) Peak position analysis of the data shown in panel (a). Error bars result from the least-squares fits of two Gaussians on top of a linear background. Yellow and green bars illustrate the peak width (vertical) and intensity (horizontal).

In a Marcus type of picture, where, in the linear response limit, the total (free) energy depends on a global solvation coordinate, the electron-transfer process from a donor state (D) to an electron acceptor (A) is characterized by the electronic coupling between these two states (Figure 4a). In the case of strong coupling, an avoided crossing causes the formation of two energy surfaces, and the system can only non-adiabatically "jump" from one (the CB) to the other (e_S) through vertical transitions in the Born–Oppenheimer limit. In

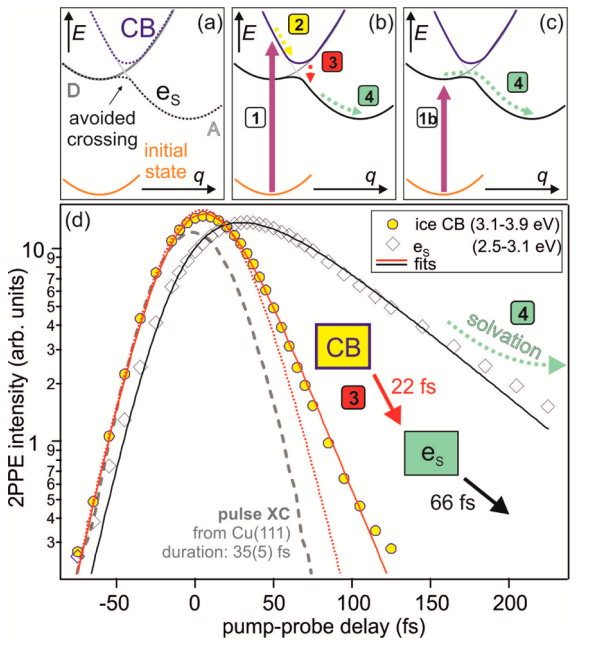

Figure 4. (a) Marcus picture in the strong coupling limit, showing the formation of two energy surfaces for CB and e_S. (b) Charge injection from the metal (1), relaxation to the CB minimum (2), vertical transition to e_S (3), and progression toward the potential minimum by solvation (4). (c) Direct excitation to e_S. (d) Time-dependent, integrated 2PPE intensity of CB (circles) and e_S (diamonds) fitted by a rate equation model (solid lines). Solid (dotted) red lines compare fits with (without) direct population of e_S.

DOI: 10.1021/ja511571y
J. Am. Chem. Soc. 2015, 137, 3520−3524

the present experiment, photoexcitation occurs from an initial state in the metal (orange curve) to the CB continuum, as illustrated in Figure 4b (1). It should be noted that the momentum distribution of the bands has been neglected in this sketch for the sake of clarity; however, it has no impact on the qualitative dynamics occurring. The system evolves adiabatically toward the minimum of the CB at VBE = 0.8 eV (2) and crosses over to e_S with a certain rate, $1/\tau_{CB}$ (3). Subsequently, the new potential minimum is reached by further solvation (4), which is reflected in the energy shift of e_S in Figure 3b. Remarkably, the experiment shows that the vertical transition between the energy surfaces goes along with a significant increase in the VBE by 420−600 meV, which shows the strength of the coupling between D and A states. This large amount of energy needs to be dissipated. One scenario is strong coupling to the molecular environment when the electrons get trapped. The energy could, for example, be released to high-frequency O−D stretch vibrations, which have an energy of $\hbar\omega$ = 300 meV (2400 cm^{-1}). A full oscillation period of this vibration is 14 fs and, thus, could be related to the ultrafast energy loss that goes along with electron trapping. However, energy dissipation to the metal substrate by an Auger type of process is also plausible, where electron−hole pairs would be generated close to the Fermi energy.[30]

The abruptness of this energy loss, occurring within only a few tens of femtoseconds, strongly suggests that electron trapping occurs at pre-existing sites, as self-trapping by half an electronvolt in such a short time seems unlikely. If the electron-trapping sites existed prior to photoexcitation, a vertical transition from the metal's initial state directly to e_S could be possible if a non-vanishing dipole matrix element for optical excitation existed. This has not been observed for ice−metal interfaces and would be an alternative to the indirect excitation pathway of electron injection through the ice CB (1) and the subsequent relaxation mechanisms (2)−(4) discussed so far. As illustrated by Figure 4c, the excited electrons could directly and adiabatically relax toward the minimum of the e_S total energy curve, thus "skipping" the detour to the CB. However, if a direct excitation (1b) of e_S were possible, it should be reflected in the population dynamics of e_S, as discussed in the following.

Characterization of the population dynamics in the CB and e_S is achieved by spectral integration of both features (CB, 2.5−3.1 eV; e_S, 3.1−3.9 eV; cf. Figure 1b) and analysis of their temporal evolution. The integrated intensity transients are plotted as a function of pump−probe time delay in Figure 4d. While the CB transient (full circles) exhibits a fast decay, the e_S transient (diamonds) exposes a delayed rise and a subsequent slower decay. Assuming a filling of e_S through the CB, the data are fitted using the simplest applicable rate equation model:[31]

$$\dot{n}_{CB} = -\frac{1}{\tau_{CB}} n_{CB} \quad \text{and} \quad \dot{n}_S = \frac{1}{\tau_{CB}} n_{CB} - \frac{1}{\tau_S} n_S \tag{1}$$

where the CB is emptied into e_S with a characteristic time constant τ_{CB}. The e_S population simultaneously decays with an average time constant τ_S to the metal substrate, which acts as a sink for the excited electron population, as shown previously.[23] This rate equation system is solved by

$$n_{CB}(t) = n^0_{CB}\, e^{-t/\tau_{CB}} \tag{2a}$$

$$n_S(t) = n^0_S\, e^{-t/\tau_S} + n^0_{CB} \frac{\tau_S}{\tau_{CB} - \tau_S} [e^{-t/\tau_{CB}} - e^{-t/\tau_S}] \tag{2b}$$

Here, $n^0{}_{CB}$ and $n^0{}_S$ denote the initial, photoexcited population in CB and e_S, respectively. Note that the second term in eq 2b describes the population dynamics in e_S due to indirect excitation through the CB, while the first term accounts for the population decay of directly excited electrons in e_S. These population functions were convoluted with the laser pulses' cross-correlation (XC) trace (gray dashed curve in Figure 4d), which represents the instrument's response function, before fitting them to the data (solid curves in Figure 4d).[32] Using τ_{CB} = 22(5) fs and τ_S = 66(5) fs, the fits reproduce the data very well up to 150 fs. At larger delays, a slowing down of the e_S population decay is observed. This is in good agreement with previous investigations that unveiled a slowing down of electron transfer to the metal substrate due to enhanced screening by the evolving solvation shell.[23]

Indeed, fitting of the 2PPE transients requires an initial occupation of e_S ($n^0_S \approx n^0_{CB} \neq 0$). On the other hand, for $n^0_S = 0$, the fit results in a considerably faster population transfer from the CB of τ_{CB} = 11(5) fs. This cannot be correct, as illustrated by the dotted red curve in Figure 4d. Hence, we conclude that photoexcitation quasi-instantaneously populates *both*, ice CB *and* e_S, and thus, the electrons are trapped at pre-existing sites in the ASW.

As the population-transfer dynamics of CB and e_S can be modeled consistently without taking into account ultrafast (<20 fs) population decay to the metal, we conclude that the highly efficient charge transfer to e_S with τ_{CB} = 22(5) fs is the rate-limiting step for CB population decay. This means that the ultrafast relaxation dynamics in the ice CB and the localization in pre-existing traps are *unaffected* by the presence of the metal, probably because they occur in the orientational band gap of Cu(111) and significantly faster than electron transfer to the metal, which is manifested in the initial population decay time constant of e_S (τ_S = 66(5) fs). Remarkably, this is in perfect agreement with the intrinsic decay time of 67 fs for excess electrons in ASW on Cu(111), determined previously by empirical model calculations.[23] It should be noted that the substrate independence can only be deduced with regard to the *population* dynamics in and out of the CB; the absolute VBE may differ for ice clusters, bulk ice, or liquid water.[33]

Beyond electronic coupling, it should be noted that possible effects of the metal substrate on the ASW *structure* (i.e., on the type of pre-existing trapping site) cannot be excluded. However, previous scanning tunneling microscopy studies[34,35] showed only a weak interaction of adsorbed D_2O on Cu(111). The ultrafast relaxation dynamics in and out of the CB observed in this work clearly show that these processes occur on a femtosecond time scale in an aqueous surrounding and that, if pre-existing traps are present, electron localization can occur in ASW as fast as 22 fs. The possibility of this efficient charge trapping might explain the lack of VBE measurements of the ice and water CB until now.

■ CONCLUSIONS

In summary, we have characterized all elementary electronic processes involved when injecting excess electrons into ASW on a metal substrate. Thereby, we observe all elementary steps during the "birth" of a SE in an aqueous surrounding in real time: Electrons are resonantly excited from the modified SS of Cu(111) to the delocalized CB and (i) relax toward the CB minimum at 800 meV VBE at an extraordinarily large rate of 4 meV/fs. This energy is, due to the delocalized character of the CB, analogous to the V_0 of bulk ice, although its absolute value

DOI: 10.1021/ja511571y
J. Am. Chem. Soc. 2015, 137, 3520−3524

might differ due to the presence of the substrate. (ii) Localization into e_S occurs within 22 fs, accompanied by a gain of several hundred meV of binding energy, which is possibly dissipated to high-frequency vibrations of the molecular environment. Dynamics on only slightly longer time scales have been reported for liquid water recently.[36] In agreement with our previous studies,[21−23,34,35] we observe continued solvation on a longer time scale. Our current results thus complement our earlier work and give a complete picture of the dynamics occurring at D_2O−metal interfaces. Besides the indirect pathway through the ice CB, we also find that e_S can be populated directly through photoexcitation of metal electrons from the Cu sp band. This observation demonstrates (iii) that these traps are pre-existing in the ASW and that e_S is not formed through self-trapping. Furthermore, we show that the electron population dynamics prior to electron solvation are unaffected by the presence of the metal substrate. This suggests that the observed ultrafast trapping dynamics can be considered as representative even for electron dynamics in and out of the CB of bulk ice and possibly liquid water.

AUTHOR INFORMATION

Corresponding Author

*staehler@fhi-berlin.mpg.de

Notes

The authors declare no competing financial interest.

ACKNOWLEDGMENTS

We thank Michael Meyer for fruitful discussions. J.-C.D. and D.W. acknowledge support by the International Max Planck Research School, *Functional Interfaces in Physics and Chemistry* and *Dynamics in New Light* Helmholtz Graduate School, respectively. Cover art enhancement performed by WERKSDESIGN.

REFERENCES

(1) Ball, P. *Chem. Rev.* **2008**, *108*, 74−108.
(2) Lu, Q. B.; Madey, T. E. *J. Chem. Phys.* **1999**, *111*, 2861.
(3) Nitzan, A. *Chemical Dynamics in Condensed Phases*; Oxford Graduate Texts, Oxford University Press: Oxford, UK, 2006.
(4) Zhu, D.; Zhang, L.; Ruther, R. E.; Hamers, R. J. *Nat. Mater.* **2013**, *12*, 836−841.
(5) Zhang, L.; Zhu, D.; Nathanson, G. M.; J. Hamers, R. J. *Angew. Chem., Int. Ed.* **2014**, *53*, 9746−9750.
(6) Petrik, N. G.; Monckton, R. J.; Koehler, S. P. K.; Kimmel, G. A. *J. Chem. Phys.* **2014**, *140*, 204710.
(7) Coe, J. V. *Int. Rev. Phys. Chem.* **2001**, *20*, 33−58.
(8) Coe, J. V.; Lee, G. H.; Eaton, J. G.; Arnold, S. T.; Sarkas, H. W.; Bowen, K. H.; Ludewigt, C.; Haberland, H.; Worsnop, D. R. *J. Chem. Phys.* **1990**, *92*, 3980.
(9) Ayotte, P.; Johnson, M. A. *J. Chem. Phys.* **1997**, *106*, 811.
(10) Hammer, N. I.; Shin, J.-W.; Headrick, J. M.; Diken, E. G.; Roscioli, J. R.; Weddle, G. H.; Johnson, M. A. *Science* **2004**, *306*, 675−679.
(11) Bragg, A. E.; Verlet, J. R. R.; Kammrath, A.; Cheshnovsky, O.; Neumark, D. M. *Science* **2004**, *306*, 669−671.
(12) Paik, D. H.; Lee, I.-R.; Yang, D. S.; Baskin, J. S.; Zewail, A. H. *Science* **2004**, *306*, 672−675.
(13) Kee, T. W.; Son, D. H.; Kambhampati, P.; Barbara, P. F. *J. Phys. Chem. A* **2001**, *105*, 8434−8439.
(14) Savolainen, J.; Uhlig, F.; Ahmed, S.; Hamm, P.; Jungwirth, P. *Nat. Chem.* **2014**, *6*, 697−701.
(15) Photoexcitation may occur directly from VB to CB (Figure 1a) or from a donor species in the solution. In both cases, it is assumed that the subsequent dynamics occur independently of the photohole and that the SE complex can be regarded as a charged H_2O ensemble.
(16) Tang, Y.; Shen, H.; Sekiguchi, K.; Kurahashi, N.; Mizuno, T.; Suzukiand, Y.-I.; Suzuki, T. *Phys. Chem. Chem. Phys.* **2010**, *12*, 3653−3655.
(17) Siefermann, K. R.; Liu, Y.; Lugovoy, E.; Link, O.; Faubel, M.; Buck, U.; Winter, B.; Abel, B. *Nat. Chem.* **2010**, *2*, 274−279.
(18) Bovensiepen, U.; Gahl, C.; Stähler, J.; Bockstedte, M.; Meyer, M.; Baletto, F.; Scandolo, S.; Zhu, X.-Y.; Rubio, A.; Wolf, M. *J. Phys. Chem. C* **2009**, *113*, 979−988.
(19) The apparent disagreement between the surface VBEs of water and ice can be rationalized by considering that they were measured 100 ps (liquid) and 10 min (solid) after electron injection, respectively.
(20) Onda, K.; Li, B.; Zhao, J.; Jordan, K. D.; Yang, J.; Petek, H. *Science* **2005**, *308*, 1154−1158.
(21) Gahl, C.; Bovensiepen, U.; Frischkorn, C.; Wolf, M. *Phys. Rev. Lett.* **2002**, *89*, 107402.
(22) Meyer, M.; Stähler, J.; Kusmierek, D. O.; Wolf, M.; Bovensiepen, U. *Phys. Chem. Chem. Phys.* **2008**, *10*, 4932−4938.
(23) Stähler, J.; Bovensiepen, U.; Gahl, C.; Wolf, M. *J. Phys. Chem. B* **2006**, *110*, 9637−9644.
(24) Due to its higher mass, D_2O can be easily distinguished from residual H_2O in the UHV chamber, which is particularly important for thermal desorption spectroscopy.
(25) Wegkamp, D.; Meyer, M.; Richter, C.; Wolf, M.; Stähler, J. *Appl. Phys. Lett.* **2013**, *103*, 151603.
(26) Hertel, T.; Knoesel, E.; Wolf, M.; Ertl, G. *Phys. Rev. Lett.* **1996**, *76*, 535.
(27) Petek, H.; Ogawa, S. *Prog. Surf. Sci.* **1997**, *56*, 239−311.
(28) Both effects may result from changes of the transfer matrix elements as well as from changes resulting from the D_2O−Cu interaction and scattering of the formerly free-electron-like SS.
(29) The intensity of the CB peak is significantly reduced within 50 fs, and its width becomes larger, as illustrated by the yellow bars in Figure 3b. At $t = 0$, the width is determined by the broadened Cu(111) SS and the CB dispersion along the surface normal direction, which is projected in the PE process. Electron relaxation leads to further broadening, suggesting an error of 200 meV for the VBE(CB) determination.
(30) The required wave function overlap for this process is reflected in the population decay dynamics on a 67 fs time scale, as determined in ref 22.
(31) Data analysis was done using rate equations based on the assumption that all coherences are lost. This is justified due to the inelastic character of the relaxation in CB and e_S, which is reflected in their energy shift.
(32) To account for electrons photoemitted in a 2PPE process via virtual states, a delta function at $t = 0$ fs was added before convolution.
(33) Electronic levels of adsorbed molecules are often pinned to E_{vac}; i.e., they have VBE very similar to that of free-standing films. Our previous work on SEs in D_2O layers on different substrates (Cu(111) and Ru(001))[23] showed a negligible effect of the metal (<100 meV).
(34) Stähler, J.; Mehlhorn, M.; Bovensiepen, U.; Meyer, M.; Kusmierek, D. O.; Morgenstern, K.; Wolf, M. *Phys. Rev. Lett.* **2007**, *98*, 206105.
(35) Gahl, C.; Bovensiepen, U.; Frischkorn, C.; Morgenstern, K.; Rieder, K.-H.; Wolf, M. *Surf. Sci.* **2003**, *108*, 532−535.
(36) Messina, F.; Bräm, O.; Cannizzo, A.; Chergui, M. *Nat. Commun.* **2014**, *4*, 2119.

DOI: 10.1021/ja511571y
J. Am. Chem. Soc. 2015, 137, 3520−3524